Rogue Waves

Article · January 2010

DOI: 10.1016/B978-012374473-9.00612-3

3 authors, including:

Kristian Dysthe
University of Bergen
80 PUBLICATIONS **3,985** CITATIONS

SEE PROFILE

Harald E. Krogstad
Norwegian University of Science and Technology
115 PUBLICATIONS **3,312** CITATIONS

SEE PROFILE

Oceanic Rogue Waves

Kristian Dysthe,[1] Harald E. Krogstad,[2] and Peter Müller[3]

[1]Department of Mathematics, University of Bergen, N-5008 Bergen, Norway

[2]Department of Mathematical Sciences, Norwegian University of Science and Technology, N-7491 Trondheim, Norway; email: Harald.Krogstad@math.ntnu.no

[3]Department of Oceanography, University of Hawaii, Honolulu, Hawaii 96822

Annu. Rev. Fluid Mech. 2008. 40:287–310

The *Annual Review of Fluid Mechanics* is online at fluid.annualreviews.org

This article's doi: 10.1146/annurev.fluid.40.111406.102203

0066-4189/08/0115-0287$20.00

Key Words

freak, extreme, statistics, physics

Abstract

Oceanic rogue waves are surface gravity waves whose wave heights are much larger than expected for the sea state. The common operational definition requires them to be at least twice as large as the significant wave height. In most circumstances, the properties of rogue waves and their probability of occurrence appear to be consistent with second-order random-wave theory. There are exceptions, although it is unclear whether these represent measurement errors or statistical flukes, or are caused by physical mechanisms not covered by the model. A clear deviation from second-order theory occurs in numerical simulations and wave-tank experiments, in which a higher frequency of occurrence of rogue waves is found in long-crested waves owing to a nonlinear instability.

1. INTRODUCTION

Freak wave: term used interchangeably with rogue wave

The term rogue or freak wave has long been used in the maritime community for waves that are much higher than expected for the sea state. Draper (1964, 1971) gave an early account of the phenomenon and introduced the terms to the scientific community, and Mallory (1974) provided the first discussion of the giant waves in the Agulhas current. He listed 12 reported hits and/or observations of abnormal waves (some of them causing severe damage) between 1952 and 1973. For the seafarer, rogue waves represent a frightening and often life-threatening phenomenon. There are many accounts of such waves hitting passenger ships (Didenkulova et al. 2006), container ships, oil tankers, fishing boats, and offshore and coastal structures, sometimes with catastrophic consequences. It is believed that more than 22 supercarriers have been lost because of rogue waves between 1969 and 1994 (**Figure 1**) (Kharif & Pelinovsky 2003).

The motivation for investigating rogue waves is clear, and the scientific community has studied the topic for some time, more intensely since 2000, including large research programs, meetings, and workshops (Müller & Henderson 2005, Olagnon & Athanassoulis 2000, Olagnon & Prevosto 2004, Prevosto & Forristall 2004, Rosenthal 2005).

Nearly all the hard evidence on rogue waves comes from oil-platform measurements. **Figure 2** presents two well-studied examples: one of the exceptional waves

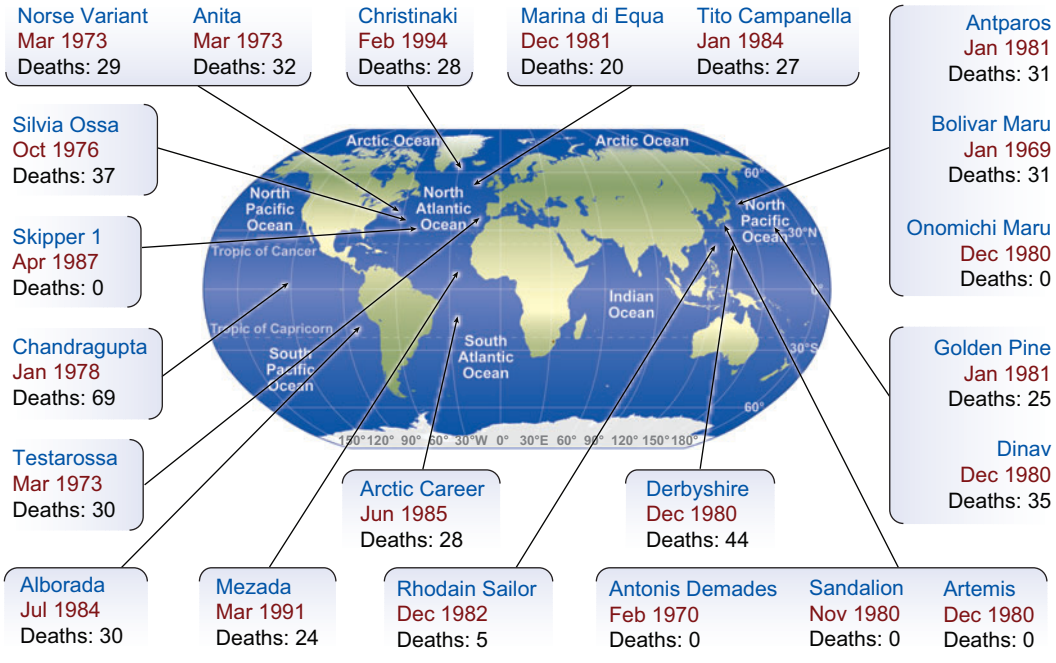

Figure 1

Locations of 22 supercarriers assumed to be lost after collisions with rogue waves between 1969 and 1994. Figure copyright C. Kharif and E. Pelinovsky, used with permission.

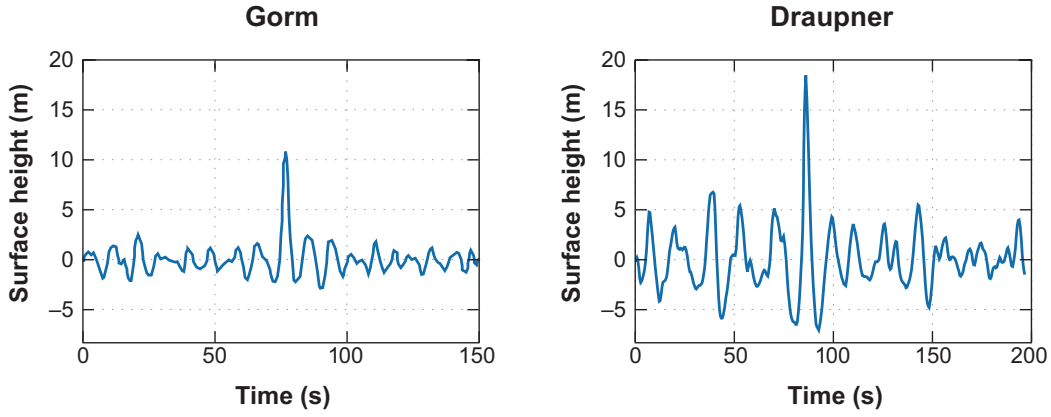

Figure 2

Two examples of rogue waves. (*Left panel*) One of the abnormal waves recorded at the Gorm field in the North Sea on November 17, 1984. The wave that stands out has a crest height of 11 m, which exceeds the significant wave height of 5 m by a factor of 2.2. (*Right panel*) The New Year wave recorded at the Draupner platform in the North Sea on January 1, 1995, at 15:20. The crest height is approximately 18.5 m and exceeds the significant wave height of 11.8 m by a factor of 1.54.

from the Gorm field in the North Sea and the New Year's wave at the Draupner platform in the North Sea.

Rogue waves are recognizable when they occur, but there is no unique definition of such waves. The pragmatic approach is to call a wave a rogue wave whenever the wave height H (distance from trough to crest) or the crest height η_c (distance from mean sea level to crest) exceeds a certain threshold related to the sea state. This review follows this practice and applies the common criteria

$$H/H_s > 2 \text{ or } \eta_c/H_s > 1.25, \quad (1)$$

where H_s is the significant wave height, here defined as four times the standard deviation of the surface elevation. **Figure 3** presents an example of the relative number of waves exceeding thresholds in H/H_s for measurements taken at the Marlin platform in the Gulf of Mexico during Hurricane Ivan. Rogue waves thus populate the tail of the probability distribution beyond $2H_s$, and in fact, not a single wave exceeded this limit for the period of recording in **Figure 3**. Nevertheless, the conditions were extreme, with H_s reaching 15.4 m and a maximum observed wave height of 26.3 m (Forristall 2005).

Researchers have attempted to determine and understand the physics of rogue waves and the probability of their occurrence. **Figure 3** includes the exceedance probabilities from Forristall's (1978) commonly used distribution and Naess's (1985) relation for a linear Gaussian sea, assuming simple storm conditions. As observed in **Figure 3**, $H/H_s > 2$ is expected to occur approximately once every 10^4 waves.

One can easily generalize linear wave theory to include interactions up to second order. It is the basic premise of this review that most rogue-wave statistics are

Wave height: total vertical distance from the wave trough (lowest point) to the wave crest (highest point)

Crest height: vertical distance from the mean water level to the crest

Significant wave height: traditionally defined as the average of the one-third largest waves and denoted $H_{1/3}$; today defined as four times the standard deviation of the surface elevation and denoted H_s

Gaussian sea: random waves in which the surface elevation has a Gaussian (normal) distribution

Linear wave theory: based on the linearized equations of water waves, traditionally used in ocean engineering and naval architecture

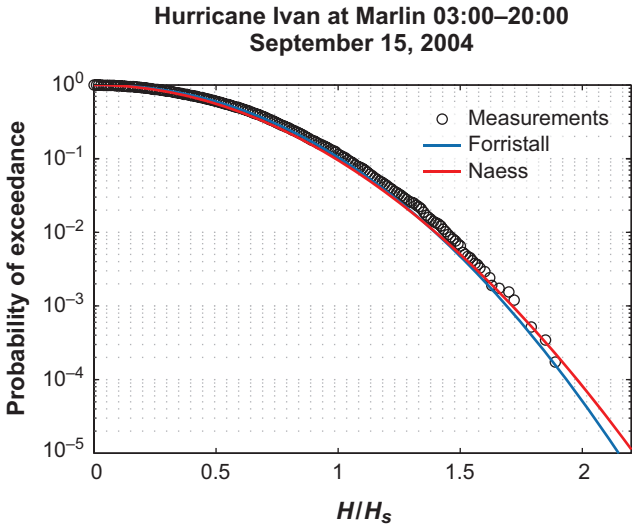

Figure 3

Observed distributions of scaled wave heights at the Marlin platform in the Gulf of Mexico during Hurricane Ivan, together with Forristall's (1978) empirical formula (*blue line*), and Naess's (1985) distribution for a narrow-band Gaussian sea (*red line*). Data provided by G.Z. Forristall.

well described by second-order random-wave theory. There are, however, observations and situations (such as waves in rapidly varying currents) that do not fit this simple paradigm and that make rogue-wave research an exciting and challenging endeavor. Presently, it is unclear whether deviations from second-order theory result from instrumental or sampling errors or require the inclusion of additional physical mechanisms in the model. Nevertheless, second-order theory serves as the benchmark when comparing against observations. The rarity of rogue waves causes sampling challenges in determining whether an observed rogue wave is consistent with a standard statistical model (Haver & Andersen 2000).

In the sections below, we describe the random models and their implications for the statistics and shape of rogue waves. We then review observations to provide some sense of their variety, and often their inconclusiveness. Finally, we explore possible physical mechanisms that might enhance the occurrence of rogue waves beyond second-order theory.

The discussion assumes some familiarity with the basic theory of water waves on the ocean and the wave spectrum (Dean & Dalrymple 1991, Tucker & Pitt 2001). The spectrum provides information about sea state and the probability distributions of wave parameters, but no information about specific individual waves.

Second-order random-wave theory: refined and more accurate than linear theory, routinely used in current ocean engineering

Wave spectrum: wave energy distribution as a function of wave number (wavelength and direction)

2. THE STATISTICS OF LARGE WAVES

2.1. Random Models of Ocean Waves

The linear (Gaussian) random model of oceanic waves is a formal superposition of elementary waves:

$$\eta(\mathbf{x}, t) = \sum_{k} a(\mathbf{k}) \cos(\mathbf{k} \cdot \mathbf{x} - \omega t + \alpha(\mathbf{k})), \qquad (2)$$

where η is the elevation, $\mathbf{x}$ is the horizontal position, and t is the time. The wave number $k = |\mathbf{k}|$ and the frequency ω satisfy the dispersion relation $\omega^2 = gk \tanh(hk)$, where g is the gravitational acceleration and h is the water depth (Dean & Dalrymple 1991). Moreover, a and α are random variables, uncorrelated for each $\mathbf{k}$. As the number of elementary waves becomes larger, η becomes Gaussian with zero mean and variance: $\sigma^2 = \int_{\mathbf{k}} \Psi(\mathbf{k}) d\mathbf{k}$, where $\int_{\Delta\mathbf{k}} \Psi(\mathbf{k}) d\mathbf{k} = \sum_{\mathbf{k}\in\Delta\mathbf{k}} \frac{1}{2} E\,|a(\mathbf{k})|^2$ defines the wave number spectrum. The wave steepness s is defined as $s = k_p \sigma$, where k_p is the wave number at the spectral peak. The steepness under storm conditions is normally less than 0.07.

Wave steepness: essentially the ratio between significant wave height and dominating wavelength

Nonlinear models are obtained by a perturbation expansion with respect to s. To second order, the elementary wave is

$$\eta(\mathbf{x}, t) = a\cos\theta + \frac{1}{2}ka^2\cos(2\theta), \quad \theta = \mathbf{k}\cdot\mathbf{x} - \omega t + \alpha. \tag{3}$$

Compared with the linear wave, this second-order wave has higher crests and shallower troughs but the same wave height. A general second-order solution for a superposition of waves as in Equation 2 is well established (Forristall 2000). The second-order contributions depend on the wave spectrum Ψ, in particular s and the directional characteristics of the waves. An explicit expression for the probability distribution of the surface elevation is not known except when the wave spectrum is narrow (Socquet-Juglard et al. 2005, Tayfun 1980).

Second-order theory does not affect the amplitude and spectrum of the free waves. This changes when the perturbation expansion is carried to third order in s. The third-order terms may now satisfy the dispersion relation and lead to resonant interactions among the free waves and a slow change in the wave spectrum with time (Hasselmann 1962).

In most circumstances, the statistical distributions of the surface elevation, wave height, and crest heights are well described by the second-order random model. Third-order resonant interactions, although important for the development of the spectrum, appear less important for the statistics of the local waves. This is supported by third-order numerical simulations, in which the surface distribution compared quite well with the second-order distribution (**Figure 4**) (Socquet-Juglard et al. 2005).

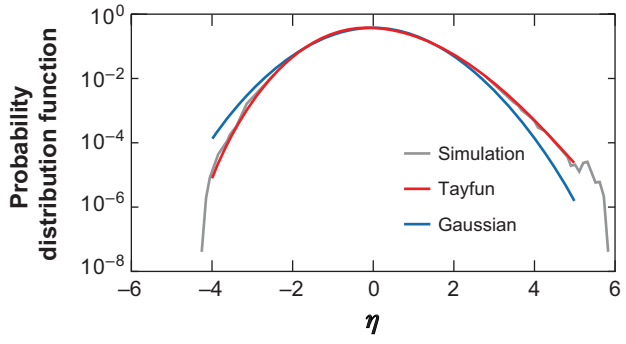

Figure 4

Distribution of the surface elevation η scaled by the standard deviation σ as simulated by a third-order model (*gray line*), compared with second-order theory, Tayfun (1980) (*red line*) and linear Gaussian theory (*blue line*).

2.2. Single-Point Extremes

Exceedance probability: probability that a random quantity exceeds a certain limit

For realistic wave fields, wave statistics expresses the wave-height exceedance probabilities in terms of Weibull distributions:

$$P(H > xH_s) = \exp(-x^{\alpha}/\beta), \tag{4}$$

where the parameters α and β depend only slightly on the sea state, at least for simple wind seas (Forristall 1978, Krogstad 1985, Naess 1985). Longuet-Higgins's (1952) seminal results for a linear, narrow-banded wave field are $\alpha = 2$ and $\beta = 1/2$.

Numerical simulations and observations suggest that one can obtain the probability distribution for the maximum wave height in a wave record containing N waves by assuming independent wave heights. It then follows from Equation 4 that the most probable maximum wave height within the record is

$$H_M = H_s(\beta \ln N)^{1/\alpha}. \tag{5}$$

The exceedance probability of the crest height η_c is also well described by Weibull distributions similar to Equation 4. However, α and β now vary significantly with some of the sea-state parameters and with the water depth (Forristall 2000, Prevosto & Forristall 2004).

Figure 5 shows the crest- and wave-height exceedance probabilities for some of the currently used expressions. Forristall's model for crest heights, based on second-order numerical simulations (Forristall 2000), shows good agreement with most observed data. The same is true for Naess's wave-height model for a Gaussian sea with a realistic spectrum and Forristall's (1978) empirical relation (cf. **Figure 3**). Although the Gaussian model severely underpredicts the probability of observing large crests, it gives reasonable predictions for the wave height. Note that Forristall's crest-height distributions depend strongly on s. Forristall's model for crest height and Naess's model for wave height compose what could be considered the standard model.

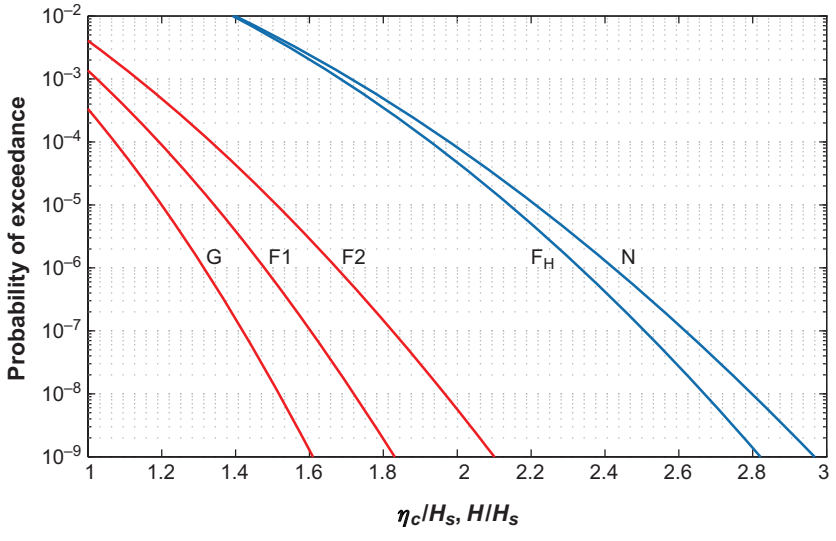

Figure 5

Probability of exceedance for crest heights (G, F1, F2) and wave heights (N, F_H). G, linear Gaussian model; F1, Forristall's (2000) second-order model for medium wave steepness; F2, Forristall's second-order model for high wave steepness; N, Naess's (1985) wave-height model for Gaussian seas and typical wind-wave spectra; F_H, Forristall's (1978) empirical wave-height model based on buoy data from the Gulf of Mexico.

According to Naess's model, the criterion $H/H_s > 2$ corresponds to an exceedance probability of approximately 10^{-4}. If one chooses the criterion $\eta_c/H_s > 1.25$, the same exceedance probability is obtained for Forristall's second-order model for medium wave steepness. Both these criteria are used interchangeably in the literature. Unfortunately, the old definition of significant wave height as the mean of the one-third largest waves is still in widespread use, and because $H_{1/3}$ is approximately 5% lower than H_s (Forristall 1978), the rogue-wave criteria have to be adjusted accordingly.

2.3. Space-Time Extremes

Whereas the extreme-value theory of wave records taken at single points has been the subject of extensive research, the corresponding theory for spatial data is less developed. The concept of wave height is not even well defined in a two-dimensional field.

However, accurate asymptotic relations exist for the maximum crest height of multidimensional Gaussian fields (Piterbarg 1996) depending on the number of waves within the region and the dimensionality. Krogstad et al. (2004) illustrate this dependence by considering a storm over an area 100 × 100 km and lasting for 6 h. With a mean wave period of 10 s, there are $N = 2160$ waves at any fixed location. For the same wave period and a directional spread of approximately 20°, one expects a mean wavelength $\lambda_p \approx 200$ m and a mean crest length $\lambda_c \approx 450$ m. Using $\lambda_p \lambda_c$ as the characteristic area of one wave, there are at each instant approximately $N = 10^5$ waves within the storm area. Applying Piterbarg's (1996) Gaussian theory for the duration of the storm, one then predicts for the expected maximum crest height $E(\eta_{\max})_{\text{time}} = 1.02 H_s$ at one particular location over a 6-h period, $E(\eta_{\max})_{\text{space}} = 1.32 H_s$ over the storm area at a fixed time, and $E(\eta_{\max})_{\text{space+time}} = 1.69 H_s$ over the storm area during the 6-h duration. These numbers differ significantly. Part of the difference results from the increase in the number of waves (corrected for space-time correlation), but it also includes a genuine dimensional effect.

2.4. The Shape of Large Waves

Mariners have described rogue waves as walls of water, pyramidal waves, and holes in the ocean. In the absence of suitable instruments for measuring surface motion over large areas, researchers have studied the three-dimensional shape of large waves using analytic methods and numerical simulations.

A useful analytical tool is the so-called Slepian model representation of a stationary Gaussian stochastic surface (Lindgren 1972). Let us consider a wave with a high maximum at $\mathbf{x} = \mathbf{0}$ at a fixed time. According to the Slepian theory, the surface $\eta(\mathbf{x})$ around the high maximum may be written as

$$\eta(\mathbf{x}) = \eta(\mathbf{0}) \frac{\rho(\mathbf{x})}{\rho(\mathbf{0})} + \Delta(\mathbf{x}), \tag{6}$$

where $\rho(\mathbf{x})$ is the covariance function, and the residual process $\Delta(\mathbf{x})$ is Gaussian with zero mean. The approximation $\eta(\mathbf{x}) \sim \eta(\mathbf{0})\rho(\mathbf{x})/\rho(\mathbf{0})$ is only reasonable in a region

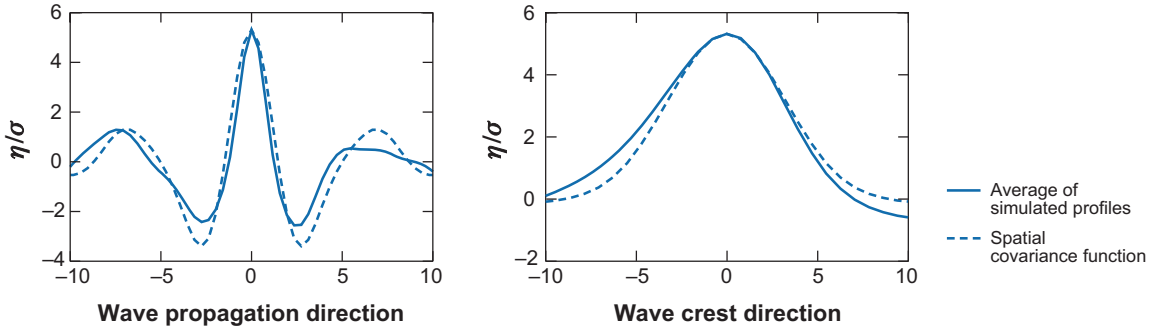

Figure 6

(*Solid line*) Averaged scaled surface profiles (in wave propagation and crest directions) of very high crests obtained from a large-scale third-order simulation of short-crested waves (Socquet-Juglard et al. 2005). (*Dashed line*) Scaled spatial covariance function (Slepian model).

in which $\Delta(\mathbf{x})$ is small, which typically surrounds the maximum out to approximately one wave/crest length. Thus, for a Gaussian surface, the average wave profile around a very high crest is that of the scaled covariance function of the field (Lindgren 1972). Owing to the Gaussian symmetry, the probability distribution of the crest height η_c is identical to that of the trough depth η_{tr}, and the average shape of a deep trough is the mirror image of the one of a high crest. The inclusion of nonlinearities destroys this symmetry (**Figure 4**), and one can expect the average shape of an extreme wave to change. Observations (Guedes Soares et al. 2003, Olagnon & van Iseghem 2000, Skourup et al. 1996) indicate that the ratio R between the extreme crest height and the nearest trough depth is scattered around $R = 2.2$.

Figure 6 compares data from large-scale third-order simulations (Socquet-Juglard et al. 2005). The simulation gives $R \simeq 2.3$, as compared with the Slepian formula, $R \simeq 1.5$.

It seems that higher-order models are significantly better in describing the average profile of large wave events than Gaussian and second-order models, as Gibson & Swan (2007) have also remarked. This contrasts with the distributions of surface elevation and crest height, which are well approximated by second-order models.

3. EXPERIMENTS AND OBSERVATIONS

3.1. Wave-Tank Experiments

Researchers have long used well-controlled experiments in wave tanks to study the development of regular and irregular waves. Most of this work deals with unidirectional waves forced to violent breaking or extreme crest heights through dispersive focusing (Longuet-Higgins 1974). Three-dimensional wave basins can carry out similar experiments using spatial focusing. The tank experiments complement theoretical studies of the surface itself (Onorato et al. 2004, 2006), as well as of the kinematics and acceleration of steep waves (Grue & Jensen 2006).

Wave tanks are also essential for testing vessels and structures in extreme and violent conditions. Modern wave-tank facilities can reconstruct accurately rogue-wave profiles from field observations and record the response of ships and structures to these waves (Clauss 1999, 2002; Clauss et al. 2006). However, most of the field wave data are point observations of three-dimensional waves, in contrast to their unidirectional reconstructions in the wave tank.

3.2. Field Measurements

In situ instrumentation that can track the surface elevation accurately includes wave staffs, laser and radar altimeters, buoys, and subsurface instruments such as pressure gauges and acoustic devices (Kahma et al. 2005). Although some instruments (in particular buoys and radars) give consistent results for the wave height, the data deviate considerably for crest heights (Krogstad & Barstow 2000). Pressure gauges and buoys give crest statistics even below Gaussian theory, whereas narrow-beam radars and laser altimeters invariably show crest heights above Gaussian theory. The differences are explained by the tendency of the lateral motion of buoys to avoid the high crests and the areal averaging that occurs for the pressure gauges and radars with broad footprints. Conversely, laser recordings may be sensitive to sea spray, and thus they may overpredict the actual crest height. The performance of several different measurement systems was compared in the WACSIS experiment at the Dutch coast and at the Tern platform in the North Sea (Forristall et al. 2004, Krogstad & Barstow 2004).

Data errors and inaccuracies are particularly serious when looking for exceptional waves in records from single instruments. Spikes in the data are prone to be mistaken for rogue-wave observations, and in addition many recording systems (e.g., the traditional wave buoys) employ mechanical and electronic filters that need to be compensated for when an accurate surface tracking is needed. Much of the published literature fails to discuss these topics in detail, and some of the published results are hard to believe.

In some exceptional cases, measurements are supported by independent and observable physical effects. This was the case for the Draupner incident (discussed further below), in which damage was reported to equipment on a temporary deck below the main deck of the platform, although the damage could not be traced to that particular wave. A similar incident happened at the North Sea Ekofisk oil field on January 3, 1984, when a wave crest smashed into and broke a light wall on the lower deck of the 2–4A platform. Kjeldsen (1984) shows photographs of the damage of this incidence and estimates the crest height to be at least 21 m above mean sea level. The significant wave height for that particular day varied from 5 m to nearly 11 m, and the incidence appears to have occurred near the maximum of the storm. Even for a significant wave height of 11 m, such a wave is quite exceptional. Although more incidents based on visual evidence have been reported, comparable waves have never been recorded by the fairly extensive wave-measuring systems at Ekofisk. Photographs of extreme waves taken from ships abound in the maritime literature, but it is difficult to derive quantitative wave parameters from such pictures.

Occurrence probability: probability that an arbitrary selected wave satisfies the rogue-wave criteria

Fixed instruments on platforms in the open sea give the most reliable information on rogue waves, although there is the disconcerting possibility that the platform itself has some influence on the recordings, as demonstrated by Forristall (2005). To provide a sense of the variety and quality of rogue-wave data, we discuss some of the measurements in detail below.

Frigg field. The wave-elevation measurements from the Plessey wave radar at the Frigg oil field in the northern North Sea (depth 106 m) compose a long-term and thoroughly quality-checked data set. Olagnon & van Iseghem (2000) considered 18,000 time series of 20-min duration (1.6×10^6 waves) for sea states with $H_s > 2$ m. The criteria $H > 2H_{1/3}$ and $\eta_c > 1.25H_{1/3}$ produced 81 and 76 rogue waves, respectively, giving a frequency of occurrence $\sim 5 \times 10^{-5}$ in both cases. This value is approximately one-third the probability inferred from **Figure 5**. Although the Frigg data contain some quite extreme height and crest ratios, the occurrence is somewhat below that of the standard model. Olagnon & van Iseghem find the ratio of the crest height to the trough depth to be scattered around 2.1 for the most extreme waves, consistent with other studies.

North Alwyn field. The wave data from the North Alwyn field (depth 128 m), less than 100 km west of Frigg, have been studied by several groups (Guedes Soares et al. 2003; Stansell 2004, 2005; Wolfram & Venugopal 2003). The instrumentation consists of three laser altimeters manufactured by Thorn EMI and mounted on different sides of the platform. Guedes Soares et al. (2003) considered 421 recordings during a storm from November 16–22, 1997, containing a total of 54,245 waves. The highest relative wave height was $2.24H_s$, which is slightly higher than the expected $2.16H_s$ for this number of waves. Similarly, the highest relative crest height according to second-order theory should be approximately $1.4H_s$ (assuming medium steepness), and three events, ranging from $1.48H_s$ to $1.58H_s$, exceed this value. Thus one might conclude that the standard model slightly underestimates the occurrence probability of the crest but not of the wave height.

Stansell (2004) considered a larger collection of 354,000 waves from North Alwyn, of which 104 exceeded the height criterion $H > 2H_{1/3}$, again slightly higher than the standard-model prediction. This paper presents a detailed plot of one exceptional wave, whose height is $3H_s$ and whose frequency of occurrence (1 in 354,400) is approximately 3000 times more than expected from second-order theory.

All the North Alwyn studies show a similar tendency, namely that although the number of waves exceeding the rogue-wave criteria by and large fit the standard model, a few waves stand out and do not seem to abide by the model. One may draw a similar conclusion from Warren et al.'s (1998) study based on data from other North Sea locations.

Gorm field. Radar altimeter data have been collected at the Gorm field in the central North Sea (depth 40 m) for years (Sand et al. 1990, Skourup et al. 1996). **Figure 7** is replotted from Hansen & Klinting (1991) using a Weibull probability scale. The maximum crest height $\eta_{\max}$ and wave height $H_{\max}$ have been extracted from 20-min

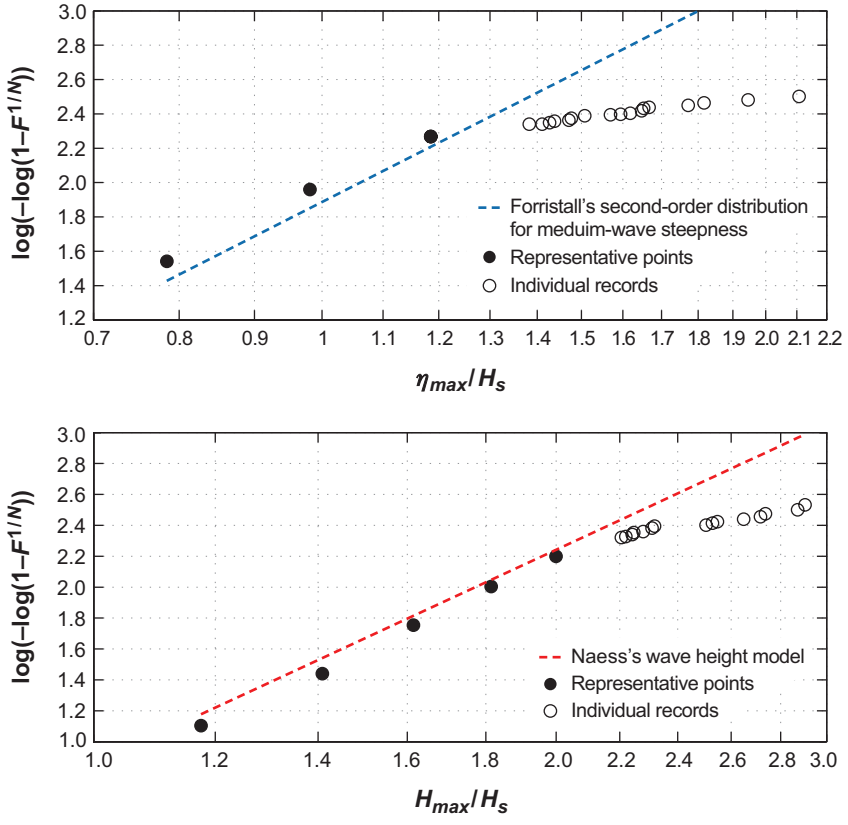

Figure 7

Empirical distribution functions of η_{max}/H_s (*upper panel*) and H_{max}/H_s (*lower panel*) for ~5000 20-min records from the Gorm field. The filled circles are representative points, whereas the open circles represent individual records. The dashed straight line on the crest-height plot (*upper panel*) is Forristall's second-order distribution for medium-wave steepness. The dashed straight line in the wave-height plot (*lower panel*) is Naess's wave-height model. Points falling below the straight lines indicate a larger frequency of occurrence.

wave records containing on the average 140 waves. The records cover significant heights up to 5 m. The distributions show signs of two different populations of waves: a normal population adhering to standard wave statistics and an exceptional population often referred to as true rogue waves.

The data contain 25 waves in which η_c/H_s ranges from 1.35 to 2.3 and 24 waves in which H/H_s ranges from 2.2 to 2.94. Note, however, that H_s is only 2–4 m for the most extreme waves. The cumulative maximum wave-height distribution appears to bend away from Naess's model at approximately $H/H_s \sim 2.1$. A similar behavior is also seen for the normalized crest height. The wave heights for the bulk of the records lie somewhat above Naess's model, whereas the crests tend to fall below Forristall's model. Nevertheless, the extreme data points clearly indicate a frequency of occurrence in excess of that predicted by standard theory.

The Draupner wave. The Draupner New Year wave occurred on January 1, 1995, and is shown in **Figure 2** (Haver 2004). It was recorded by a laser instrument at an unmanned satellite platform, and, as noted above, minor damage on a temporary deck below the main deck supports the reading. The crest height is 18.5 m above the mean water level and the wave height is 26 m. The significant wave height is estimated to

be approximately 12 m so that $\eta_c / H_s \simeq 1.54$. Second-order theory gives a probability of exceedance of approximately 2×10^{-6}, which for this particular sea state amounts to a return period of approximately 2.3 months.

Campos Basin, Brazil. Our examples above are platform measurements, but there are also a few studies involving buoy measurements. Pinho et al. (2004) investigated 7457 17-min time series (1.2×10^6 waves) from a Datawell Waverec^{TM} directional buoy moored in deep water in the Campos Basin off the coast of Brazil. The criterion $H_{max}/H_{1/3} > 2$ resulted in 108 waves from the zero downcrossing and 197 waves from the zero upcrossing analysis, roughly in accordance with the standard theory prediction of 160 waves. The most extreme ratio in the study was $H_{max}/H_s = 2.54$, slightly higher than expected from standard theory. However, buoy measurements, although proven quite reliable for estimates of spectra and sea-state parameters, are generally believed to be less accurate for detailed wave profiles.

Japanese measurements. Several Japanese research groups have reported rogue-wave analyses of data from long-term wave measurements around Japan. The measuring device, situated on the sea bed at approximately 50 m depth, is an ultrasonic wave gauge originally developed by the Ship and Harbor Research Institute in the 1960s and today manufactured by Kaijo Sonic Corporation. The instrument as well as the data processing have undergone considerable development over the years, but the accuracy of the surface detection and horizontal averaging and other details of the signal processing are not known to us.

Tomita & Kawamura (2000) present a statistical analysis of data from the Yura test site offshore Japan. Although showing two wave records with impressive single waves, their analysis is difficult to compare with other analyses because of a different definition of a genuine freak wave. Mori et al. (2002) have published several studies of data from a location where three ultrasonic wave gauges are located close enough to each other to carry out some cross-validation. These studies give a general picture that is not so different from the Gorm field measurements discussed above. The wave crests follow a fitted Edgeworth-Rayleigh distribution (Mori & Yasuda 2002) up to about the rogue-wave criterion above which measured crests are higher than predicted. A similar effect is seen for wave height, which follows Naess's and Forristall's distributions for the bulk of the data.

True rogue waves? Several studies show far more extraordinary waves than those discussed above, but the quality of their data cannot be inferred from the publications. Divinsky et al. (2004) present a Datawell Waverider record from the Black Sea in a medium sea state with $H_s = 2.6$ m. Apart from pronounced wave groups, the record also displays one extreme wave with a crest height of 8.9 m and a total wave height equal to 10.32 m. A thorough inspection of the instrument has not disclosed any malfunctioning (L. Lopatukhin, personal communication).

Liu & MacHutchon (2006) have also reported spectacular possible rogue-wave measurements from a gas-drilling platform offshore South Africa southwest of the Agulhas current. They obtained these measurements from a Marex wave radar with standard sampling. Unfortunately, only overall wave parameters such as H_s and H_{max}

have been retained for each record, but the data set contains values for H_{max} up to 10 times H_s (one single case gave a ratio of more than 20, which exceeds the physical limitations of the system). During the WACSIS intercomparison project, the Marex radar produced markedly higher crests than the other systems (Forristall et al. 2004), and the authors are aware of this fact and are rather cautious in their conclusions.

The overall impression from the observations is that most of them are consistent with the standard statistical model, but there are, after a careful assessment of the quality of the data, observations that are hard to rationalize within this framework. It is also a contentious statistical issue as to what can and cannot be inferred from a single observation that is far out on the tail of an assumed probability distribution. If there are indeed deviations from the standard theory, then one needs to inquire about possible additional physical mechanisms.

3.3. Satellite and Radar Measurements of Rogue Waves

Spaceborne synthetic aperture radar (SAR) is currently the only instrument that has the capacity of observing large spatial wave fields with single-wave resolution. Even though a SAR image looks similar to an ordinary photographic image of the ocean surface, it is far from being so. The imaging mechanism is highly nonlinear, with the surface velocity contributing significantly to the image modulation through a velocity-dependent displacement of the surface scatterers. This leads to a strong attenuation in the imaging of waves traveling along the satellite flight direction and represents a serious limitation of the system.

Recently, a research group from the German Aerospace Center tried to obtain the surface elevation itself from SAR data (Schulz-Stellenfleth & Lehner 2004). The algorithm, still under development, has occasionally produced surfaces showing extremely high waves. Even if the limitations of the procedure are fully recognized by the research group, the possibility of measuring rogue waves globally from a satellite has excited the media. The major problem with developing a reliable algorithm based on SAR is the lack of ground-truth data for intercomparison and validation. This problem and simplifications in the current algorithm are the reasons why the research group has been met with vigorous scientific opposition (Janssen & Alpers 2006). At the time of this writing, the SAR-based wave-height estimates are far from validated, and the media's excitement may be unjustified. Nevertheless, the potential of using satellites for global surveillance of the world's oceans is considerable, and even if it turns out to be difficult or even impossible to map the surface height by the present satellite SARs, it may be possible to develop some rogue-wave signatures from the radar data.

A marine radar, situated on a high coastal cliff, or preferably on an offshore platform, is another way to obtain the surface elevation. There are severe theoretical obstacles in this case as well, and current research still has some way to go before the technique can be used operationally (Dankert & Rosenthal 2004).

4. PHYSICAL MECHANISMS

Rogue waves represent a very high local concentration of wave energy compared with the average of the field, and a number of mechanisms are known to produce

large waves from moderately small ones: spatial focusing, dispersive focusing, and nonlinear focusing.

4.1. Spatial Focusing

Spatial focusing can be achieved by the refraction of waves in varying bottom topography or in variable currents. As waves propagate into shallower water and their wavelength becomes comparable to the water depth, the waves get refracted, and they align their crests with the topography and steepen. Along irregular coastlines, this might lead to the focusing of wave energy in particular places, which may provide suitable locations for wave power devices (Halliday & Dorrell 2004).

The giant waves in the Agulhas current off the African southeast coast, a notorious example of current refraction, have received a lot of attention (Grundlingh 1994; Irvine & Tilley 1988; Lavrenov 1998, 2003; Mallory 1974; Peregrine 1976; Smith 1976). Between Durban and East London, the current has a jetlike structure running in a southwesterly direction along the shelf edge. Researchers have observed the occurrence of abnormal waves in connection with the passage of cold fronts followed by strong winds and waves from the southwest. Lavrenov (1998) showed that it is possible for waves moving upstream to become trapped in the jet as it widens south of East London (see **Figure 8**). Meanders of the current may be another source of wave trapping (Irvine & Tilley 1988). As a result, the sea state within the jet becomes more severe than outside, and such an increase has been observed (Grundlingh 1994, Irvine & Tilley 1988). Lavrenov (1998) used a numerical model to reconstruct the

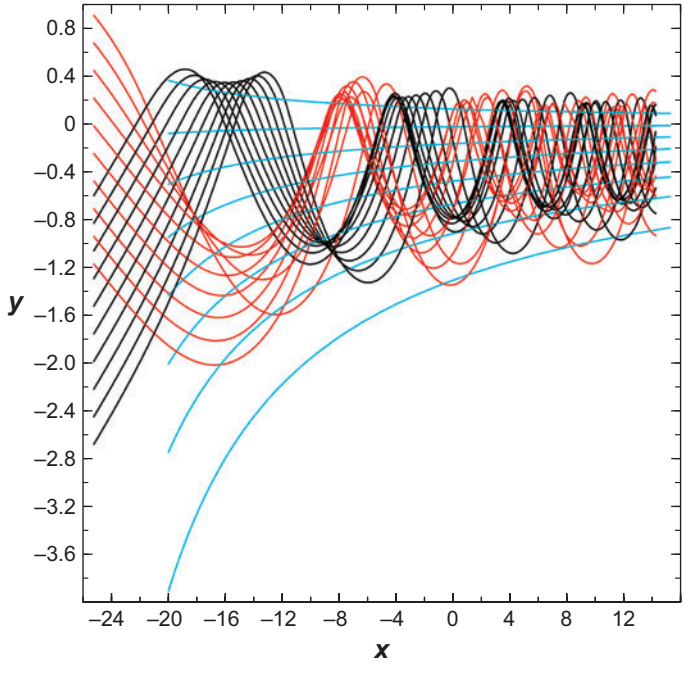

Figure 8

Rays of waves moving upstream into a widening current jet. The current field (*blue streamlines*) is similar to that of Lavrenov (1998) for the Agulhas current. On the figure, the unit on both axes is equal to 40 km. The red and black families of rays correspond to 10-s waves with an initial 20° difference in propagation directions.

wave spectrum within the current from a given swell spectrum outside. The estimated increase in H_s up to 100% is in fair agreement with satellite measurements (Grundlingh 1994).

As seen in **Figure 8**, if the incoming waves are unidirectional, their entrapment also produces caustics near the reflection zones. Peregrine (1976) and Smith (1976) suggested that giant waves could be explained by wave amplification at such caustics. Even though a small directional spread of the incoming waves tends to smear out the caustics, this mechanism may still be relevant when almost unidirectional swell enters the current. Refraction in the geometric optics approximation only describes changes in the spectrum of the waves and breaks down near caustics. The incident and reflected waves then become phase locked and are described by Airy functions. It is this change of wave form near the caustics that might give rise to exceptional waves. To study such rogue-wave formation, one thus needs to employ analytical methods beyond geometric optics or rely on direct numerical simulations.

White & Fornberg (1998) used ray tracing to study refraction of initially unidirectional waves entering random currents with velocity fluctuations of the order of 10 cm s^{-1}, typical of mid-ocean eddies. Such random eddies can give focusing provided their scale is sufficiently large ($\geq$10 km). However, even a small angular spread tends to smear out the caustics (Dysthe 2000). Heller (2005) revisited White & Fornberg's (1998) work using a more realistic simulation model with waves entering the eddy field now having a small angular spread $\Delta\theta$. Although the caustics were indeed smeared out, there were still fluctuations and hot spots in the wave energy density, provided that the typical angular deflection $\delta\theta$ of a ray passing through an eddy was larger than $\Delta\theta$. However, order-of-magnitude estimates based on group velocity, vorticity, and correlation distance reveal that $\delta\theta \sim 5°$, which is smaller than the typical angular spread of a storm-wave spectrum.

4.2. Dispersive Focusing

Gravity waves are dispersive with phase and group velocities inversely proportional to the frequency. This effect is applied in a well-known technique, first suggested by Longuet-Higgins (1974), to produce short groups of large waves at a given position in a wave tank. The idea is to create a long wave group with linearly decreasing frequency, known as a chirp. With proper design of the chirp, dispersion forces this group to contract to a few wavelengths at a given position. This type of focusing has also been suggested as a possible mechanism for exceptional rogue waves [see the review by Kharif & Pelinovsky (2003), and references therein]. If a given chirped wave train produces strong focusing in the absence of other waves, it will still do so, although somewhat weaker, when superimposed in a random-wave field. If the amplitude of the deterministic chirped wave train is below the standard deviation of the surface, it remains invisible until it focuses.

The dispersive focusing is a linear effect and occurs even in a linear Gaussian sea in those rare circumstances in which waves happen to have the contrived phase relations necessary to form a chirped wave train. Physical mechanisms able to produce such phase relations and chirped wave trains have not been identified for the ocean.

4.3. Nonlinear Focusing

Nonlinear focusing is currently the most active research topic in rogue wave formation. It is studied theoretically, numerically, and experimentally (in wave tanks), in the hope that it might provide the key to forecasting the occurrence of true rogue waves. In this section we discuss the basic physical mechanism, the Benjamin-Feir instability, and numerical simulations to assess the circumstances under which nonlinear focusing leads to the occurrence of rogue waves in excess of standard theory.

Benjamin-Feir instability. A regular periodic wave train of frequency ω and amplitude a is unstable to modulations, known as the so-called Benjamin-Feir (BF) instability (e.g., see Lake et al. 1977). Sidebands $\omega \pm \Delta\omega$ grow provided

$$\frac{\Delta\omega}{\omega} < \sqrt{2}ka. \tag{7}$$

As the instability develops with time scale $(ka)^{-2}$ wave periods, the wave train disintegrates into groups and produces some very large isolated waves. A number of authors (Clamond & Grue 2002, Henderson et al. 1999, Lake et al. 1977, Tanaka 1990, Zakharov et al. 2006) have investigated this development by means of two-dimensional numerical simulations. As groups are formed by the instability, further focusing takes place within the group, producing a very large wave having a surface elevation $\eta_{\max}$ more than three times the initial amplitude a of the wave train. Because the extreme wave has grown at the expense of the other waves in the group, it appears gigantic. Experimental investigations (Melville 1982, Su & Green 1985, Tulin & Waseda 1999) have found qualitatively similar effects, with $\eta_{\max}/a$ somewhat below 3.

For narrow spectra, the surface elevation may be represented as

$$\begin{aligned} \eta &= 2\mathrm{Re}\{A(\mathbf{x},t)\exp(i\theta) + A_2(\mathbf{x},t)\exp(2i\theta) + A_3(\mathbf{x},t)\exp(3i\theta)\}, \\ \theta &= \mathbf{k}_p\mathbf{x} - \omega(\mathbf{k}_p), \end{aligned} \tag{8}$$

where the amplitudes A, A_2, and A_3 are slowly varying. Expressed in scaled variables, the modified nonlinear Schrödinger (MNLS) equation,

$$iA_t + L_2A - \frac{1}{2}|A|^2A = (L_2 - L_5)A + \frac{i}{4}\left(7|A|^2A_x - A|A|_x^2\right) + A\bar{\varphi}_x, \tag{9}$$

governs the space-time evolution of A to $\mathcal{O}(s^3)$ and is valid for $\Delta\omega/\omega_p = \mathcal{O}\left(s^{1/2}\right)$ (Dysthe 1979; Lo & Mei 1985, 1987; Trulsen & Dysthe 1996; Trulsen et al. 2000). The potential $\bar{\varphi}$ represents the flow generated by the nonuniformity of the wave stress and satisfies $\nabla^2\bar{\varphi} = 0$, with $\bar{\varphi}_z = |A|_x^2/2$ at $z = 0$, and the L_n operators are Taylor expansions to order n in ∂_x and ∂_y of $[(1-\partial_x)^2 - \partial_y^2]^{1/4} - 1$. When the spectrum is very narrow, $\Delta\omega/\omega_p = \mathcal{O}(s)$, the right-hand side of Equation 9 is $\mathcal{O}(s^4)$, and the nonlinear Schrödinger (NLS) equation is recovered to $\mathcal{O}(s^3)$.

In two dimensions, the NLS equation has some simple exact solutions that have been associated with rogue-wave phenomena, namely the envelope soliton, $A(x,t) = a\exp(-ia^2t/4)/\cosh(ax)$, and the breathers, the simplest one found by

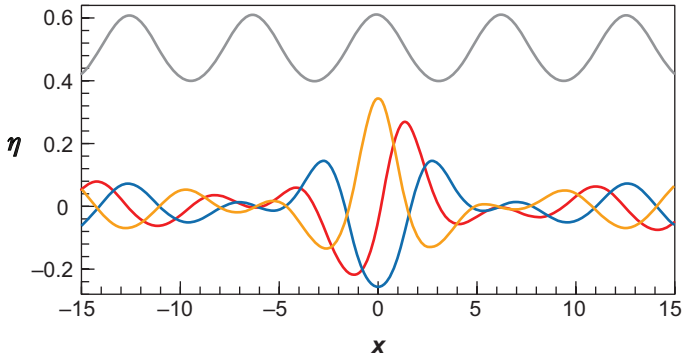

Figure 9

Development of a breather. On a time scale of s^{-2} wave periods, a regular wave train (*top*) develops into an extreme group (*bottom*), of which three snapshots during a half–wave period are shown.

Peregrine (1983),

$$A(x,\, t) \,=\, a \exp\left(-i\frac{a^2 t}{2}\right)\left(1 - \frac{4(1 - ia^2 t)}{1 + 8a^2x^2 + a^4t^2}\right), \quad a > 0, \tag{10}$$

both written in the group velocity frame. Tending to a uniform wave train when $t \to \pm\infty$, Equation 10 develops a narrow group, with the largest wave having a crest height $\eta_{\max}$ that is more than three times the initial (and final) amplitude a when t passes through zero (**Figure 9**). Henderson et al. (1999) found that the breather solution gave a reasonable approximation to their steep wave events in fully nonlinear simulations (see also Clamond et al. 2006, Dysthe & Trulsen 1999).

Although impressive waves can be achieved through the BF-type instability, the initial states from which they develop are highly unlikely to occur spontaneously in storm-generated waves. However, Alber (1978) showed that a BF-type instability persisted in a narrow-band random-wave field provided that the relative bandwidth satisfied $\Delta\omega/\omega_p < 2s$. The ratio $BFI = 2s/(\Delta\omega/\omega_p)$ is called the BF index (Janssen 2003). Storm-wave spectra typically have $BFI < 1$. Theory and simulations in two dimensions (Dysthe et al. 2003, Janssen 2003, Mori & Yasuda 2000, Onorato et al. 2000) have shown that spectra with $BFI > 1$ are unstable and develop on the BF time scale toward marginal stability. While the instability develops, the population of rogue waves increases. Onorato et al. (2006) have verified this increase experimentally in a long wave flume. Although this suggests that the BF instability can produce rogue waves in excess of the standard statistics, three-dimensional simulations indicate that this only occurs for very long-crested waves (Gramstad & Trulsen 2007).

Three-dimensional numerical simulations. Ideally, one would like to simulate the full Euler equations describing the ocean surface in a large area. Such a simulation requires huge computational resources, but it is being attempted, e.g., by Tanaka (2001).

There are various ways to lower the computational burden. One way is to use relatively small computational domains but contrive the initial conditions to assure the development of large waves (e.g., see Gibbs & Taylor 2005, Gibson & Swan 2007).

To study the spontaneous development of extreme waves, one needs a computational domain containing thousands of waves, thus requiring approximations to the full Euler equations. Although most storm-wave spectra are reasonably narrow

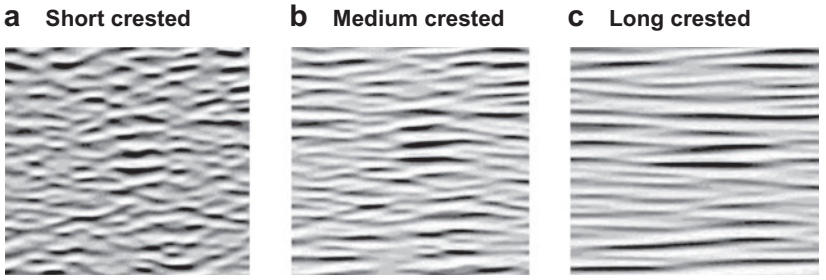

Figure 10

Excerpts of simulated surfaces from a large-scale third-order simulation (Socquet-Juglard et al. 2005). Approximately 2% of the computational domain is shown at an early stage of the simulation for a (*a*) short-, (*b*) medium-, and (*c*) long-crested case.

banded, the NLS equation, requiring the relative spectral width $\Delta\omega/\omega_p = \mathcal{O}(s)$, has turned out to be too restrictive. The MNLS equation (Equation 9) reduces the narrow-band requirement to $\Delta\omega/\omega_p = \mathcal{O}(s^{1/2})$. Quantitative comparisons of the MNLS equation with experiments and fully nonlinear simulations have shown it to be a good approximation for times up to $(\omega_p s^3)^{-1}$. Using the MNLS equations, Socquet-Juglard et al. (2005) have made simulations with a computational domain containing approximately 10^4 waves. The simulations were initiated with truncated JONSWAP spectra with three different angular distributions: short-, medium-, and long-crested waves. **Figure 10** shows tiny sections of the simulated surfaces after a few periods. The BF index is larger than one for all three cases, and the spectrum evolves on the BF time scale, most pronounced for the long-crested case.

Because of the size of the computational domain, the probability of exceedance of the crest height can be well estimated at any time in the evolution process. For

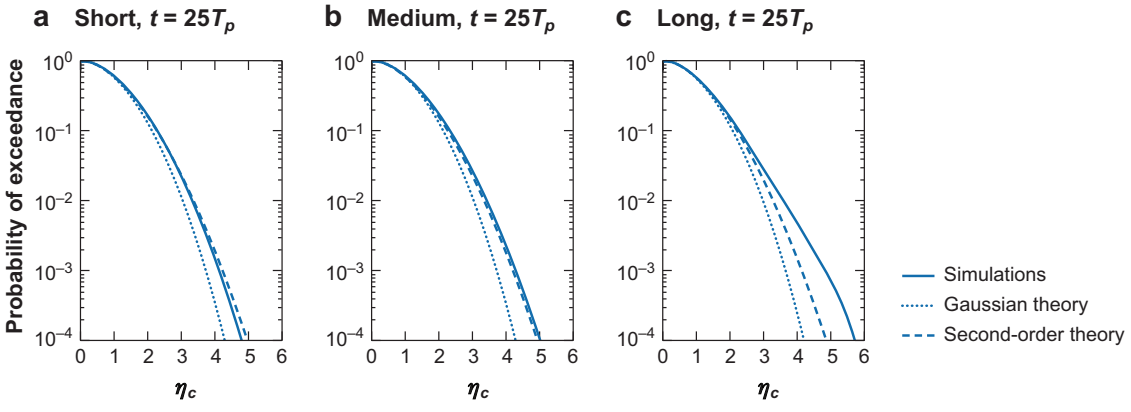

Figure 11

Probability of exceedance of the crest height η_c (scaled by the standard deviation σ) for the short-, medium-, and long-crested cases in **Figure 10*a–c***, respectively, at the time $t = 25T_p$ when the Benjamin-Feir instability is developing. Full line represents simulations; dotted line represents Gaussian theory; and dashed line represents second-order theory.

short- and medium-crested cases, there is no significant change, and the probability is well approximated by the second-order prediction. However, in the long-crested case, a significant increase in the probability of large waves is found during the BF-instability phase. **Figure 11** shows the probability of exceedance of the normalized crest height for the three cases presented in **Figure 10** after 25 wave periods.

The statistics of the long-crested case are in good agreement with the experimental results of Onorato et al. (2006). Gramstad & Trulsen (2007) have performed a much larger number of these simulations and find a sharp qualitative transition in the occurrence of large waves when the average crest length exceeds approximately 10 wavelengths.

5. CONCLUSIONS

In this article, rogue waves are waves that satisfy one or both criteria in Equation 1. The standard statistical model assumes that rogue waves result from random superposition in a sea of weakly (up to second-order) interacting waves. The standard model predicts the surface elevation distribution, the crest- and wave-height distributions, the exceedance probabilities, and the wave forms as a function of sea state. Except for the wave forms that seem to be better predicted by higher-order theory, most observations of rogue waves are consistent with this standard model. Rogue waves in excess of those predicted by standard theory are often called true rogue waves. There is no generally accepted explanation or theory for the occurrence of such true rogue waves. There seems, however, to be a consensus among researchers that if true rogue waves do occur in strong currents (such as the Agulhas current off the eastern coast of South Africa) or in coastal waters, they are most likely caused by refractive focusing. True rogue waves might also exist in the open ocean far away from strong current gradients or topography, although reasonable doubt about the reliability of some of the measurements and observations is still warranted. At present, the only viable mechanism to generate true rogue waves in the open ocean is a modification of the BF instability limited, however, to very long-crested sea. The usual rogue waves result from random superposition, and they cannot be predicted from the wave spectrum in any deterministic fashion. Because the underlying physical mechanisms for the generation of true rogue waves have not clearly been identified, there is also no generally accepted prediction scheme for these, although in the Agulhas current, the warning is to stay clear of the current when cold fronts with high winds are approaching from the southwest. Progress is expected to come from a combination of more reliable measurements, extensive field observations, careful statistical analysis, and numerical simulations. Tank experiments are of vital importance for the engineering community, but their controlled circumstances might not pay proper tribute to the uncontrollable nature of rogue waves in the open sea.

DISCLOSURE STATEMENT

The authors are not aware of any biases that might be perceived as affecting the objectivity of this review.

ACKNOWLEDGMENTS

Peter Müller wishes to thank Chris Garrett for insightful discussions. We also thank Dr. George Z. Forristall for providing the wave data from Hurricane Ivan and Dr. Søren P. Kjeldsen for valuable input about the Ekofisk incidence on January 3, 1984.

LITERATURE CITED

Alber IE. 1978. The effects of randomness on the stability of two-dimensional surface wavetrains. *Proc. R. Soc. London A* 363:525–46

Clamond D, Francius M, Grue J, Kharif C. 2006. Long time interaction of solitons and freak wave formations. *Eur. J. Mech. B* 25:536–53

Clamond D, Grue J. 2002. Interaction between envelope solitons as a model for freak wave formations. Part I: long time interaction. *C. R. Mec.* 330:575–80

Clauss G, Schmittner C, Klein M. 2006. Generation of rogue waves with predefined steepness. *Proc. 25th Int. Conf. Offshore Mech. Arctic Eng., June 4–9, Hamburg, Germany*, Pap. no. OMAE2006-92272. New York: ASME

Clauss GF. 1999. Task-related wave groups for seakeeping tests or simulation of design storm waves. *Appl. Ocean Res.* 21:219–34

Clauss GF. 2002. Dramas of the sea: episodic waves and their impact on offshore structures. *Appl. Ocean Res.* 24:147–61

Dankert H, Rosenthal W. 2004. Ocean surface determination from X-band radar-image sequences. *J. Geophys. Res.* 109:C04016

Dean RG, Dalrymple RA. 1991. *Water Wave Mechanics for Engineers and Scientists*. Singapore, World Sci. 368 pp.

Didenkulova II, Slunyaev AV, Pelinovsky EN, Kharif C. 2006. Freak waves in 2005. *Nat. Hazards Earth Syst. Sci.* 6:1007–15

Divinsky BV, Levin BV, Lopatukhin LI, Pelinovsky EN, Slyunyaev AV. 2004. A freak wave in the Black Sea: observations and simulation. *Dokl. Earth Sci.* 395:A438–43

Draper L. 1964. "Freak" ocean waves. *Oceanus* 10:13–15

Draper L. 1971. Severe wave conditions at sea. *J. Inst. Navig.* 24:273–77

Dysthe KB. 1979. Note on a modification to the nonlinear Schrödinger equation for application to deep water waves. *Proc. R. Soc. London* A 369:105–14

Dysthe KB. 2000. Modelling a "rogue wave": speculations or a realistic possibility? See Olagnon & van Iseghem 2000, pp. 255–64

Dysthe KB, Trulsen K. 1999. Note on breather type solutions of the NLS as model for freak waves. *Phys. Scr.* 82:T48–52

Dysthe KB, Trulsen K, Krogstad HE, Socquet-Juglard H. 2003. Evolution of a narrow-band spectrum of random surface gravity waves. *J. Fluid Mech.* 478:1–10

Forristall GZ. 1978. On the distributions of wave heights in a storm. *J. Geophys. Res.* 83:2353–58

Forristall GZ. 2000. Wave crest distributions: observations and second order theory. *J. Phys. Ocean.* 30:1931–43

Forristall GZ. 2005. Understanding rogue waves: Are new physics really necessary? See Müller & Henderson 2005

Forristall GZ, Barstow SS, Krogstad HE, Prevosto M, Taylor PH, Tromans P. 2004. Wave crest sensor intercomparison study: an overview of WACSIS. *J. Offshore Mech. Arct. Eng.* 126:6–34

Gibbs RH, Taylor PH. 2005. Formation of walls of water in 'fully' nonlinear simulations. *Appl. Ocean Res.* 27:142–57

Gibson RS, Swan C. 2007. The evolution of large ocean waves: the role of local and rapid spectral changes. *Proc. R. Soc. A* 463:21–48

Gramstad O, Trulsen K. 2007. Influence of crest and group length on the occurrence of freak waves. *J. Fluid Mech.* 82:463–72

Grue J, Jensen A. 2006. Experimental velocities and accelerations in very steep wave events in deep water. *Eur. J. Mech. B* 25:554–64

Grundlingh ML. 1994. TOPEX/Poseidon observes wave enhancement in the Agulhas current. *AVISO Altimeter Newsl.* 3

Guedes Soares C, Cherneva Z, Antão EM. 2003. Characteristics of abnormal waves in the North Sea storm sea states. *Appl. Ocean Res.* 25:337–44

Halliday JR, Dorrell DG. 2004. Review of wave energy resource and wave generator development in the UK and the rest of the world. *Proc. Eur. Power Energy Syst.*, Art. no. 442–136

Hansen NEO, Klinting P. 1991. Design freak waves. Dan. Hydraul. Inst. & LIC Rep., Copenhagen

Hasselmann K. 1962. On the nonlinear energy transfer in a gravity wave spectrum. 1. General theory. *J. Fluid Mech.* 12:481–500

Haver S. 2004. A possible freak wave event measured at the Draupner Jacket January 1 1995. *Proc. Rogue Waves 20–22 October*. Brest: IFREMER

Haver S, Andersen OJ. 2000. Freak waves, rare realizations of a typical population or a typical realization of a rare population. *Proc. 10th Int. Offshore Polar Eng. Conf. Seattle*, 3:123–30. Cupertino, CA: ISOPE

Heller E. 2005. Freak waves: just bad luck, or avoidable? *Europhys. News* 2005(5):159–62

Henderson KL, Peregrine DH, Dold JW. 1999. Unsteady water wave modulations: fully nonlinear solutions and comparison with the NLS equation. *Wave Motion* 29:341–61

Irvine DE, Tilley DG. 1988. Ocean wave directional spectra and wave-current interaction in the Agulhas from the shuttle imaging radar-B synthetic aperture radar. *J. Geophys. Res.* 93:15389–401

Janssen PAEM. 2003. Nonlinear four wave interaction and freak waves. *J. Phys. Ocean* 33:863–84

Janssen PAEM, Alpers W. 2006. Why SAR wave mode data of ERS and Envisat are inadequate for giving the probability of occurrence of freak waves. *Proc. SEASAR Workshop, 23–26 January, ESA SP-613, Frascati, Italy.* **http://earth.esa.int/workshops/seasar2006/proceedings/**

Kahma K, Hauser D, Krogstad HE, Lehner S, Monbaliu JAJ, Wyatt LR, eds. 2005. *Measuring and Analysing the Directional Spectrum of Ocean Waves*. Luxembourg: EU COST Action 714, EUR21367. 465 pp.

Kharif C, Pelinovsky E. 2003. Physical mechanisms of the rogue wave phenomenon. *Eur. J. Mech. B* 22:603–34

Kjeldsen SP. 1984. Dangerous wave groups. *Nor. Marit. Res.* 1984(2):4–16
Krogstad HE. 1985. Height and period distributions of extreme waves. *Appl. Ocean Res.* 7:158–65
Krogstad HE, Barstow SF. 2000. A unified approach to extreme value analysis of ocean waves. *Proc. 10th Int. Offshore Polar Eng. Conf., Seattle*, 3:103–8. Cupertino, CA: ISOPE
Krogstad HE, Barstow SF. 2004. Analysis and applications of second order models for the maximum crest height. *J. Offshore Mech. Arct. Eng.* 126:66–71
Krogstad HE, Liu J, Socquet-Juglard H, Dysthe KB, Trulsen K. 2004. Spatial extreme value analysis of nonlinear simulations of random surface waves. *Proc. 23rd Int. Conf. Offshore Mech. Arct.* Eng., *20–25 June*, *Vancouver*, Pap. no. OMAE2004–51336. New York: ASME
Lake BM, Yuen HC, Rungaldier H, Ferguson WE. 1977. Nonlinear deep-water waves: theory and experiment. Part 2: evolution of a continuous wave train. *J. Fluid Mech.* 83:49–74
Lavrenov I. 1998. The wave energy concentration at the Agulhas current of South Africa. *Nat. Hazards* 17:117–27
Lavrenov I. 2003. *Wind-Waves in Oceans*. Berlin: Springer-Verlag
Lindgren G. 1972. Local maxima of Gaussian fields. *Ark. Mat.* 10:195–218
Liu C, MacHutchon KR. 2006. Are there different kinds of rogue waves? *Proc. Int. Conf. Offshore Mech. Arct. Eng., June 4–9, Hamburg*, Pap. no. OMAE2006-92619. New York: ASME
Lo EY, Mei CC. 1985. A numerical study of water-wave modulation based on a higher-order nonlinear Schrödinger equation. *J. Fluid Mech.* 150:395–416
Lo EY, Mei CC. 1987. Slow evolution of nonlinear deep water waves in two horizontal directions: a numerical study. *Wave Motion* 9:245–59
Longuet-Higgins MS. 1952. On the statistical distribution of the heights of sea waves. *J. Mar. Res.* 11:245–65
Longuet-Higgins MS. 1974. Breaking waves in deep and shallow water. *Proc. 10th Symp. Nav. Hydrodyn.*, pp. 597–605. Cambridge, MA: Office Naval Res.
Mallory JK. 1974. Abnormal waves in the south-east coast of South Africa. *Int. Hydrog. Rev.* 51:89–129
Melville WK. 1982. The instability and breaking of deep-water waves. *J. Fluid Mech.* 115:165–85
Mori N, Liu PC, Yasuda T. 2002. Analysis of freak wave measurements in the Sea of Japan. *Ocean Eng.* 29:1399–414
Mori N, Yasuda T. 2000. Effects of high-order nonlinear wave-wave interactions on gravity waves. See Olagnon & van Iseghem 2000, pp. 229–44
Mori N, Yasuda. 2002. A weakly non-Gaussian model of wave height distribution for random wave train. *Ocean Eng.* 29:1219–31
Müller P, Henderson D, eds. 2005. *Rogue Waves. Proc., 14th 'Aha Huliko' Hawaii. Winter Workshop, Univ. of Hawaii Manoa*, Honolulu: School of Ocean Earth Sci. Technol., Spec. Publ. 193 pp. **http://www.soest.hawaii.edu/PubServices/AhaHulikoa.html**
Naess A. 1985. On the distribution of crest to trough wave heights. *Ocean Eng.* 12:221–34

Olagnon M, Athanassoulis G, eds. 2000. *Rogue Waves 2000: Proceedings of Workshop*. Brest: IFREMER

Olagnon M, Prevosto M, eds. 2004. *Rogue Waves 2004: Proceedings of Workshop*. Brest: IFREMER. **http://www.ifremer.fr/web-com/stw2004/rw/**

Olagnon M, van Iseghem S. 2000. Some observed characteristics of sea states with extreme waves. *Proc. 10th Int. Offshore Polar Eng. Conf. ISOPE, Seattle*, 3:84–90. Cupertino, CA: ISOPE

Onorato M, Osborne AR, Serio M, Cavaleri L, Brandini C, Stansberg CT. 2004. Observation of strongly non-Gaussian statistics for random sea surface gravity waves in wave flume experiments. *Phys. Rev.* 70:067302

Onorato M, Osborne AR, Serio M, Damiani T. 2000. Occurrence of freak waves from envelope equations in random ocean wave simulations. See Olagnon & van Iseghem 2000, pp. 181–91

Onorato M, Osborne AR, Serio M, Caavaleri L, Brandini C, Stansbert CT. 2006. Extreme waves, modulational instability and second order theory: wave flume experiments on irregular waves. *Eur. J. Mech. B Fluids* 25:586–601

Peregrine DH. 1976. Interaction of water waves and current. *Adv. Appl. Mech.* 16:9–117

Peregrine DH. 1983. Water waves, nonlinear Schroedinger equations and their solutions. *J. Aust. Math. Soc. B* 25:16–43

Pinho UF, Liu PC, Ribeira CEP. 2004. Freak waves at Campos Basin, Brazil. *Geofizika* 21:53–66

Piterbarg VI. 1996. *Asymptotic Methods in the Theory of Gaussian Processes and Fields*. Transl. Math. Monogr., Vol. 148. Providence, RI: Am. Math. Soc.

Prevosto M, Forristall GZ. 2004. Statistics of wave crests from models vs. measurements. *J. Offshore Mech. Arct. Eng.* 126:43–50

Rosenthal W. 2005. Results of the MAXWAVE project. See Müller & Henderson 2005

Sand SE, Hansen NEO, Klinting P, Gudmestad OT, Sterndorff M. 1990. Freak wave kinematics. In *Water Wave Kinematics*, ed. A Torum, OT Gudmestad, pp. 535–49. NATO ASI Series E: Appl. Sci., Vol. 178. Dordrecht: Kluwer Acad.

Schulz-Stellenfleth J, Lehner S. 2004. Measurement of 2-D sea surface elevation fields using complex synthetic aperture radar data. *IEEE Trans. Geosci. Remote Sens.* 42:1149–60

Skourup J, Andreasen KK, Hansen NEO. 1996. Non-Gaussian extreme waves in the central North Sea. *Proc. Int. Conf. Offshore Mech. Arct. Eng., 1A, June 16–20, Florence*. New York: ASME

Smith R. 1976. Giant waves. *J. Fluid Mech.* 77:417–31

Socquet-Juglard H, Dysthe KB, Trulsen K, Krogstad HE, Liu J. 2005. Probability distributions of surface gravity waves during spectral changes. *J. Fluid Mech.* 542:195–216

Stansell P. 2004. Distributions of freak wave heights measured in the North Sea. *Appl. Ocean Res.* 26:35–48

Stansell P. 2005. Distributions of extreme wave, crest and trough heights measured in the North Sea. *Ocean Eng.* 32:1015–36

Su MY, Green AW. 1985. Wave breaking and nonlinear instability coupling. In *The Ocean Surface: Wave Breaking, Turbulent Mixing, and Radio Probing*, ed. Y Toba, H Mitsuyasu, pp. 31–38. Dordrecht: Reidel

Tanaka M. 1990. Maximum amplitude of modulated wavetrain. *Wave Motion* 12:559–68

Tanaka M. 2001. Verification of Hasselman's energy transfer among surface gravity waves by direct numerical simulations of primitive equations. *J. Fluid Mech.* 444:199–221

Tayfun MA. 1980. Narrow-band nonlinear sea waves. *J. Geophys. Res.* 85:1548–52

Tomita H, Kawamura T. 2000. Statistical analysis and inference from the in-situ data of the sea of Japan with reference to abnormal and/or freak waves. *Proc. Int. Offshore Polar Eng. Conf.*, *Seattle*, 3:116–22. Cupertino, CA: ISOPE

Trulsen K, Dysthe KB. 1996. A modified nonlinear Schrödinger equation for broader bandwidth gravity waves on deep water. *Wave Motion* 24:281–89

Trulsen K, Kliakhandler I, Dysthe KB, Verlarde MG. 2000. On weakly nonlinear modulation of waves on deep water. *Phys. Fluids* 12:2432–37

Tucker MJ, Pitt EG. 2001. *Waves in Ocean Engineering*. Vol. 5, Ocean Eng. Book Series. Amsterdam: Elsevier. 521 pp.

Tulin MP, Waseda T. 1999. Laboratory observations of wave group evolution, including breaking effects. *J. Fluid Mech.* 378:197–232

Warren SJ, Bole JB, Driver BD. 1998. Measured wave crest distributions in central and southern North Sea storms. *Proc. ISOPE* 3:96–102

White BS, Fornberg B. 1998. On the chance of freak waves at sea. *J. Fluid Mech.* 355:113–38

Wolfram J, Venugopal V. 2003. Crest height statistics of storm waves in deep water. *Proc. Inst. Mech. Eng. M* 217:213–29

Zakharov VE, Dyachenko AI, Prokofiev AO. 2006. Freak waves as nonlinear stages of Stokes wave modulation instability. *Eur. J. Mech. B Fluids* 25:667–92

Annual Review of
Fluid Mechanics

Volume 40, 2008

Contents

Indexes

Errata

An online log of corrections to *Annual Review of Fluid Mechanics* articles may be found at http://fluid.annualreviews.org/errata.shtml